

Efficient Computational Models for the Optimal Representation of Correlated Regional Hazard

Vasileios Christou

Research Assistant, Department of Civil and Environmental Engineering, ATLSS Engineering Research Center, Lehigh University, Bethlehem, PA, USA

Paolo Bocchini

Assistant Professor, Department of Civil and Environmental Engineering, ATLSS Engineering Research Center, Lehigh University, Bethlehem, PA, USA

ABSTRACT: In this paper, a methodology is presented for the generation of an optimal set of maps representing the intensity of a natural disaster over a region. In regional hazard and loss analysis, maps like these are commonly used to compute the probability of exceeding certain levels of intensity at all sites, while also providing information on the correlation among the intensity at any pair of sites. The information on the spatial correlation between two locations is of utmost importance for the accurate disaster performance assessment of lifeline components and of distributed systems. However, traditional hazard maps (such as those provided by USGS) do not provide this essential information, but only the probability of exceedance of a specific intensity at the various sites, considered individually. Therefore, many researches have attempted to address this problem and incorporate correlation in their models, mainly with two basic approaches. The first approach includes analytic or computational methodologies to assess directly the correlation; the second approach is adopted by techniques for the selection of a representative set of intensity maps, often referred to as “regional hazard-consistent maps”. The methodology presented herein, which branches out from the previous two approaches, considers the intensity maps as random fields. By adopting this abstract perspective, the new methodology is particularly appropriate for a multi-hazard approach, and it can take advantage of tools for the optimal sampling of multi-dimensional stochastic functions. These tools ensure that the weighted ensemble of generated samples (i.e., intensity maps) tends to match all the probabilistic properties of the field, including the correlation. In fact, the samples generated by the proposed methodology fully capture the marginal hazard at each location and the correlated regional hazard. After the technique is presented, an application is provided, for the case of seismic ground motion intensity maps.

1. INTRODUCTION

During the last decades, the increased attention for socio-economic impacts of extreme events has led structural engineers to slowly shift focus from individual structures to spatially distributed systems and entire communities. Problems involving network reliability, direct structural loss estimation, and lifeline resilience are characterized by large uncertainties and strong correlation among the various physical quantities and locations. Many hazard models for various types of disasters can suc-

cessfully capture the uncertainty, but do not consider the spatial correlation. However, it has been shown that underestimating the importance of the regional correlation may introduce significant inaccuracy on the socio-economic effects. For example, Lee and Kiremidjian (2007) argued that seismic risk models that do not consider ground motion and damage correlation underestimate system risk and, as a consequence, high-cost economic decisions may end up being nonconservative. Similarly, Bocchini and Frangopol (2011) showed that

the assumption of totally uncorrelated bridge damage states in a network reliability analysis leads to large nonconservative errors on the network performance. Moreover, Crowley and Bommer (2006) demonstrated that assuming perfect spatial correlation leads to errors on the opposite side and overestimates the loss exceedance curves when a probabilistic seismic hazard analysis (PSHA) is applied.

So, it has been established, that the studies on these problems should be performed at the regional scale and the models used should take into account accurate information on the spatial correlation. This is particularly true for the correlation of the intensity measure (IM) representing the severity of a natural disaster at various locations. However, this information is not included in the most popular hazard maps, such as those provided by the United States Geological Service (USGS) for seismic hazard, and the National Oceanic and Atmospheric Administration (NOAA) for weather-related hazards. Traditional hazard maps provide information only on the marginal hazard at each site, treated individually. The techniques used to generate these maps take into account all the possible events of different intensity, occurring at different sites and with different probability, and integrate them to determine the probability of exceeding any level of a representative intensity measure (e.g., peak ground acceleration for earthquakes; wind speed for hurricanes). The drawback, however, is that the information on the fact that each event affects concurrently multiple locations is not embedded in the maps.

Therefore, the scientific community has tried to address these issues with two different approaches. The first group of researchers developed techniques which tried to assess the regional correlation in a direct fashion. In particular, a subgroup of this family used analytic techniques (Moghtaderi-Zadeh and Kiureghian, 1983; Gardoni et al., 2003), whereas some others exploited computational approaches (Bocchini and Frangopol, 2011). Even though most of this techniques are elegant and easy to implement, providing closed-form solutions, they usually have to make substantial simplifications and assumptions, which may not be realistic. The second group of scientists utilizes simulation-based

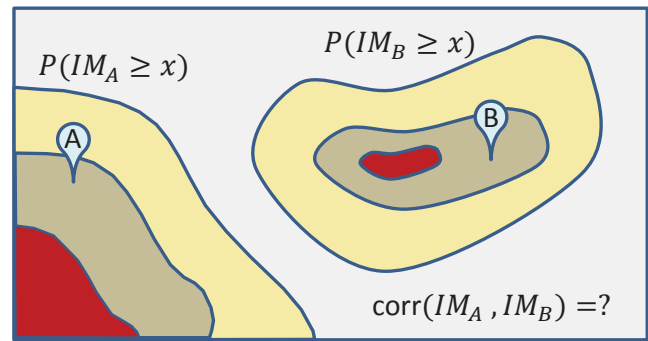


Figure 1: Hazard maps provide the marginal hazard at all points, but not their correlation.

techniques to adequately correlate the IM at various sites. This line of research led to the popular “hazard-consistent” techniques for regional intensity maps, extensively reviewed by Han and Davidson (2012) and Vaziri et al. (2012). The basic idea is to select a reduced set from a large suit of historical and/or synthetic maps, generated by selected scenario events (e.g., earthquakes). These models select and weight the maps of the reduced set in a way to match the hazard at each individual site (provided by USGS for example), as closely as possible (hence the name “hazard-consistent”).

This paper proposes to approach the problem with a different perspective. The first basic idea is to consider the IM of an extreme event over a region as a two-dimensional random field. Then, an effective technique called “Functional Quantization” (Luschgy and Pagès, 2002; Miranda and Bocchini, 2015) is used to generate a small set of maps that provide an optimal approximation (in the mean-square sense) of the desired random field. This new approach provides a very elegant formulation of the problem and enables a truly multi-hazard paradigm, because it treats in the same way the intensities of all possible disasters. In fact, the methodology requires only to have an appropriate subroutine for the simulation of IM maps for the considered hazard, such as earthquake, flood, or hurricane.

2. REPRESENTATIVE IM MAPS

For risk, loss, and resilience analyses at the community level, the problems are very complex and simulation-based approaches have arisen as the most popular option. Given the nested layers of

uncertainties (e.g., hazard, structural response, recovery phase) the total probability theorem is usually applied to split the problem in simpler tasks. Therefore, to handle the uncertainty in the hazard, the generation of a set of representative IM maps is the first step.

The selection of an appropriate IM (or a vector of IM's) and the generation of maps of its values depends on the type of analysis that is performed. For instance, in seismology it is customary to sample a few random parameters that describe the characteristics of the earthquake event, propagate the seismic effects through the region by means of attenuation functions (which could also include random parameters), and sometimes superimpose random residuals to the resulting map, to account for all the other uncertainties that are not explicitly modeled (see, for instance, Jayaram and Baker, 2010). The most common IM's are the peak ground acceleration, values of the spectral acceleration for certain periods, or a combination of these. Similarly, for hurricanes the generation of IM maps starts with the identification of a genesis point, sampling from a kernel smoothed probability distribution of the historical genesis points. Then, the hurricane track is propagated over the time steps, usually based on random parameters. Finally, the distribution of the winds is assessed at each time step, using the current location and trajectory of the hurricane, along with another set of deterministic or random parameters. Simulators that follow this scheme have been developed by Emanuel et al. (2006) and by Vickery et al. (2000), among others. In this case, a representative IM could be the maximum wind speed experienced by each site. Similar approaches can be followed for other types of disasters, such as tornadoes or floods. The IM maps generated in this way are then used as input for the subsequent analyses.

As for all probabilistic assessments, Monte Carlo simulation (MCS) can be considered as the benchmark approach. If a sufficiently large number of maps are used, MCS can accurately represent the marginal hazard at each location, as well as the spatial correlation among sites (embedded in the IM maps). However, for practical applications, the number of samples to obtain a good probabilistic

representation of the marginal hazard is at least in the order of 10^4 and to capture the correlation this number may have to increase by at least an order of magnitude. Therefore, as for many applications, the drawback of MCS is its high computational cost, which makes it impractical in most cases.

Han and Davidson (2012) have reviewed a family of methodologies that address explicitly this issue. They aim at carefully selecting a set of historical or synthetic IM maps and then applying appropriate probabilistic weights, so that the regional hazard is correctly represented even using a small number of samples ("hazard-consistent" methods).

The most prominent methodologies of this group are based on importance sampling, k-mean clustering, and optimization. Importance sampling is used to partition the large range of the hazard model parameters in a more controlled way. For example, the magnitude of the event is preferably sampled at higher values (Kiremidjian et al., 2007). This methodology improves the accuracy of a standard MCS, but in many cases is applied only to some of the parameters, ignoring other relevant ones (e.g., the source of the event).

K-mean clustering, as well as other clustering techniques, is used to group the intensity maps in clusters (Jayaram and Baker, 2010). In this case, each map is assigned to the cluster with the closest centroid map, according to the Euclidean norm. Within each iteration, the centroid of each cluster is recalculated as the mean of all the sample maps. Finally, the iterative scheme stops when no more reassignments take place and a random map is selected from each cluster. This overall approach presents many similarities with the technique that is proposed herein and will be presented in Section 3. However, the proposed technique has been developed starting from a completely different perspective, and its outcome has been proved to be optimal in the mean square sense (ideal for hazard analysis), which is not the case for previously developed techniques.

A third set of methodologies is based on probabilistic optimization. This group of techniques tries to minimize the error between the marginal hazard yielded by a set of selected IM maps and the "ex-

act” values (e.g., those provided by USGS) for a selected grid of points in a region. These optimization models have been applied to different hazards, such as earthquakes (Vaziri et al., 2012) and hurricanes (Apivatanagul et al., 2011).

Overall, these methods yield good results in terms of capturing the marginal hazard with a lower computational cost than MCS. However, they do not address explicitly the way in which the spatial correlation is modeled, which should be the main motivation for the development of most of these methodologies. The implicit assumption is that the use of real or realistic realization of the IM maps, which individually carry a spatial correlation, will automatically transfer a good representation of the correlation to the weighted ensemble. Instead, the technique proposed in the next section addresses this point explicitly, and not only optimizes the representation of the marginal hazard, but also of the the spatial correlation.

3. HAZARD QUANTIZATION METHOD

The Hazard Quantization (HQ) method diverges from the techniques previously described and approaches the regional hazard problem from another perspective. The key difference is that it embraces the nature of IM maps as random fields, which was only sporadically hinted at, in the previous literature (see, for instance, Jayaram and Baker, 2009). This approach yields several benefits. First, it allows to take direct advantage of several methodologies that have already been developed for the enhanced representation of generic random fields, and which are backed up by proofs of optimality. Second, it allows a more elegant treatment of the various quantities involved in the problem. An example of this is the fact that for the case of earthquakes, there is no distinction between the random parameters that define the earthquake source (often called “scenario parameters”) and those who model the inter- and intra-event variability (often referred to as “residuals”). HQ considers all parameters in the same way, without the need of a hierarchy and specialized simulation techniques for each group of them (which can be included, but do not need to be). This in turn yields the third advantage of HQ. Its general perspective makes it a perfect paradigm

for multi-hazard analysis. All potential causes of disasters can be addressed in the same way, with a consistent and uniform framework, where the only subroutine that is hazard-specific is the one for the generation of individual maps, as described in Section 2.

3.1. Theoretical foundation

Functional Quantization (FQ) is a technique for the optimal representation of random functions with a small number of samples (Luschgy and Pagès, 2002). FQ has strong similarities with other techniques that share the same goal, such as the Stochastic Reduced Order Models (Grigoriu, 2009). What characterizes FQ is its optimality criterion, which is the mean square convergence of the approximate representation to the actual random function. This makes it particularly appropriate for hazard analysis in general, and regional IM maps in particular, where convergence is sought on both marginal distribution and correlation.

To take advantage of FQ, the IM map is considered a stochastic function F , which is a bimeasurable random field on a given probability space $(\Omega, \mathcal{F}, \mathbb{P})$ and is defined as:

$$F(\mathbf{x}, \omega) : \Xi \times \Omega \rightarrow \mathbb{R} \quad (1)$$

where Ξ is the (multi-dimensional) space domain and Ω is the sample space.

On the other hand, the random function F_N , which approximates F , is defined by the following equation:

$$F_N(\mathbf{x}, \omega) = \sum_{i=1}^N f_i(\mathbf{x}) \cdot 1_{\Omega_i}(\omega) \quad (2)$$

where the deterministic functions $f_i(\mathbf{x})$ are called “quanta” and 1_{Ω_i} is the indicator function associated with event $\Omega_i \subset \Omega$

$$1_{\Omega_i}(\omega) = \begin{cases} 1, & \text{if } \omega \in \Omega_i \\ 0, & \text{otherwise} \end{cases} \quad (3)$$

Theoretically, almost all the probability space Ω is partitioned into a mutually exclusive and collectively exhaustive set $\{\Omega_i\}_{i=1}^N$ and each event Ω_i has an associate probability $\mathbb{P}(\Omega_i)$ and a quantum f_i ,

representative of all the sample functions associated with ω 's which belong to the event Ω_i .

The same concept can be also visualized from another perspective. This is the space of square integrable functions $L^2(\Xi)$ where the realizations of F and F_N lie. From this perspective, the $L^2(\Xi)$ space is tasseled into $\{V_i\}_{i=1}^N$, where each tassel V_i collects all the realizations $F(\omega)$ with $\omega \in \Omega_i$. Each point $f(\mathbf{x})$ in the Hilbert space $L^2(\Xi)$ can be associated with its pre-image in the probability space, hence by extension a tassel V_i matches an event Ω_i .

Thus, when FQ is utilized, operating in both the Hilbert and probability spaces, a tessellation $\{V_i\}_{i=1}^N$ and a corresponding partition $\{\Omega_i\}_{i=1}^N$ are induced. Next, the probability $\mathbb{P}(\Omega_i)$ associated with each event must be computed. However, thanks to the mentioned relationship between the two spaces, it is possible to compute instead the probability $\mathbb{P}_F(V_i) = p_i$ of the corresponding tassel V_i , which is equal to the associated $\mathbb{P}(\Omega_i)$ (Miranda and Bocchini, 2015). The set of pairs including the quanta $f_i(\mathbf{x})$ and associated probabilities p_i is called ‘‘quantizer’’, and it can be used as input for the weighted simulation of the uncertain problem.

From a practical point of view, there are several techniques to compute the quantizer of a certain random function. In particular, one technique is able to generate quantizers also for non-Gaussian, non-stationary, multi-dimensional random fields, which is what is needed for HQ. This technique is called ‘‘Functional Quantization by Infinite-Dimensional Centroidal Voronoi Tessellation’’ (FQ-IDCVT) and it extends the idea of Voronoi Tessellation (VT). VT is a technique for the partitioning of a finite-dimensional Euclidean space \mathbb{R}^n into regions $\{T_i\}_{i=1}^N$, called ‘‘Voronoi tassels’’. Each tassel is a n -dimensional convex polyhedron with a generating point $\check{\mathbf{y}}_i \in \mathbb{R}^n$ and is defined as:

$$T_i = \left\{ \mathbf{y} \in \mathbb{R}^n \mid \|\mathbf{y} - \check{\mathbf{y}}_i\| < \|\mathbf{y} - \check{\mathbf{y}}_j\| \right. \\ \left. \text{for } j = 1, 2, \dots, N; j \neq i \right\} \quad (4)$$

where $\|\cdot\|$ is the Euclidean norm. According to Equation (4), all the points $\mathbf{y} \in \mathbb{R}^n$ that belong to tassel T_i are closer to the generating point $\check{\mathbf{y}}_i$ than to

any other generating point $\check{\mathbf{y}}_{j \neq i}$. A special case of VT is the Centroidal Voronoi Tessellation (CVT), where each generating point $\check{\mathbf{y}}_i$ is also the centroid of tassel V_i . A CVT can be computed using Lloyd's Method (Ju et al., 2002).

FQ-IDCVT extends Lloyd's Method to the infinite dimensional Hilbert space of squared-integrable functions $L^2(\Xi)$ (for more details on the mathematical derivations, see Miranda and Bocchini, 2015). In the infinite-dimensional space, tassels are defined as follows:

$$T_i = \left\{ F(\omega) \in L^2(\Xi) \mid \right. \\ \left. \|F(\omega) - \check{f}_i\|_{L^2(\Xi)} < \|F(\omega) - \check{f}_j\|_{L^2(\Xi)} \right. \\ \left. \text{for } j = 1, 2, \dots, N; j \neq i \right\} \quad (5)$$

where \check{f}_i is the generating point of tassel T_i and $\|\cdot\|_{L^2(\Xi)}$ is the $L^2(\Xi)$ norm. Equation 5 denotes that all the realizations $F(\omega)$ closer to \check{f}_i than to any other $\check{f}_{j \neq i}$ are clustered in T_i . Note that the tassels generated by the CVT in Equation 5 will be used as the V_i in the FQ sense. In other words, $T_i \equiv V_i$.

The \check{f}_i 's are determined by the iterative algorithm in Figure 2 (Miranda and Bocchini, 2013) until convergence is met in terms of the following error metric named ‘‘distortion’’:

$$\Delta(\{V_i, f_i\}_{i=1}^N) = \sum_{i=1}^N \int_{V_i} \|F(\omega) - f_i\|_{L^2(\Xi)}^2 d\mathbb{P}_F \quad (6)$$

Miranda and Bocchini (2015) proved that the minimization of the distortion as defined in Equation (6) ensures that a CVT of $L^2(\Xi)$ is obtained and it is optimal according to the mean square criterion. Note that the argument of the norm in Equation (6) imposes convergence of the approximate representation to the random field, not focusing only on the first moment or the marginal distribution.

FQ-IDCVT has been shown to work particularly well against the curse of dimensionality that arises in these problems and has been demonstrated for Gaussian and non-Gaussian random fields (Christou et al., 2014; Bocchini et al., 2014). Therefore, it is used in the proposed methodology for the simulation of the strongly non-Gaussian, non-stationary, two-dimensional field representing the IM distribution over a region.

3.2. Computational algorithm

Figure 2 shows the flowchart of the FQ-IDCVT algorithm, consisting of four blocks, which are detailed in the following. The first block includes the required input data. These are: (i) probabilistic characteristics of the stochastic parameters required to generate an IM map; (ii) parameter N that is the number of sample IM maps that will be used, called “quantizer size”, which depends on the computational resources; (iii) computational parameter N_{sim} , which is usually in the order of $N_{sim} = 100 \cdot N$; (iv) N sample IM maps, which are used as the initial set of quanta.

The second module consists of the quanta identification, and it iterates the following tasks:

- generation of N_{sim} sample intensity maps;
- computation of the $L^2(\Xi)$ distance of IM map realization j from all the quanta $\{f_i\}_{i=1}^N$ in the 2D space;
- clustering of each realization j to the tassel m , where f_m is the quanta with the smallest $L^2(\Xi)$ distance from j ;
- averaging of samples in each tassel V_i and updating of the respective generating point f_i .

The third block assesses the probabilistic weights associated with the quanta, and it performs the following four steps:

- generation of Np_{sim} new sample IM maps, where usually $Np_{sim} = 10 \cdot N_{sim}$
- computation of the $L^2(\Xi)$ distances and clustering, as done in the previous block;
- assessment of the probability $\mathbb{P}(\Omega_i)$ as

$$\mathbb{P}(\Omega_i) = p_i = \frac{N_i}{Np_{sim}} \quad (7)$$

where N_i is the number of maps in cluster i .

The last block represents the output quantizer, which is the representative small set of IM maps f_i (i.e., quanta) and the associated weights p_i .

The optimal partition of the sample space Ω provided by FQ-IDCVT has been proven to be optimal and practically unaffected by the initial selection of quanta (Miranda and Bocchini, 2015). The algorithm is easy to implement and in the following numerical example it is shown that the resulting ensemble of IM maps approximates very accurately the exact marginal hazard and regional correlation.

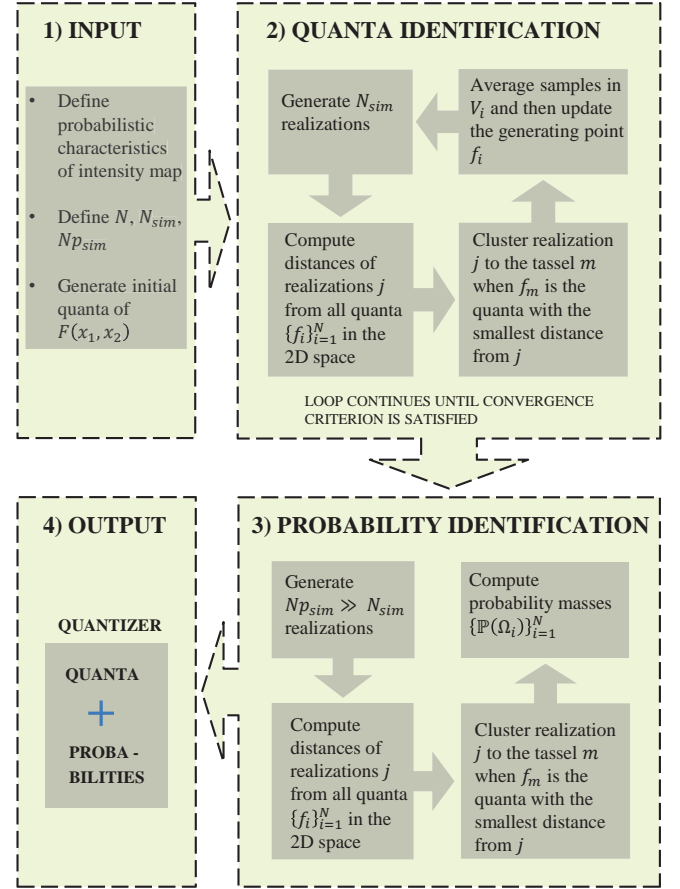


Figure 2: Flowchart of the FQ-IDCVT algorithm.

4. APPLICATION

For the demonstration of the proposed methodology, a simplified representation of an earthquake ground motion is considered. Figure 3 shows the region of interest with two predefined faults. The magnitude of the earthquake and the hypocenter depth are assumed to have a triangular distribution with minimum, mode, and maximum equal to [5.5, 6, 6.5] and [2.0, 4.0, 6.0] km, respectively. The fault type is considered strike slip and the fault rupture length is determined according to the model adopted by HAZUS-MH (DHS, 2003). In terms of attenuation, the empirical regression model presented by Abrahamson and Silva (1997) is utilized for the generation of ground shaking maps, which are in terms of spectral acceleration at a period T .

The case study is analyzed using HQ and the characteristics of the resulting quantizer are compared to the exact values of the autocorrelation and the marginal probability of exceeding a certain

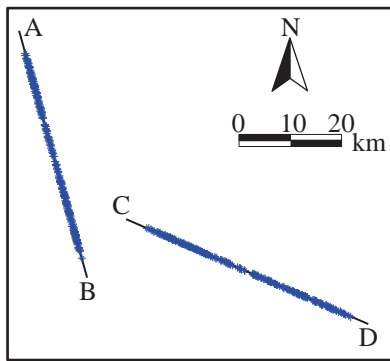


Figure 3: Specified faults AB and CD in the region of interest. The blue crosses represent the sample epicenters.

value of $S_a(T = 0.1s)$ computed by extensive MCS. The FQ-IDCVT parameters considered herein are $N = 500$, $N_{sim} = 100 \cdot N$ and $Np_{sim} = 1,000 \cdot N$.

Figure 4 shows the marginal hazard $P[S_a(T = 0.1s) > 0.4g]$. The probabilities obtained by HQ are in close agreement with the exact. Comparably good results have been obtained also for the other values of spectral acceleration threshold and period T , even at the tails of the marginal distribution.

The autocorrelation of the quantizer has been determined for different 1D stripes of the random field, to be able to plot it (the complete autocorrelation is a 4D function). An example is shown in Figure 5a. Figure 5b illustrates the difference between the ensemble autocorrelation of the quantizer and the exact. The error on this second-order statistic, which is notoriously difficult to capture, is considerably small, in the order of 0.1%.

5. CONCLUSIONS

A new methodology is presented for the generation of an optimal set of maps representing the intensity of a natural disaster over a region. The proposed approach is rooted in the idea of considering explicitly the IM maps of any hazard as a two-dimensional random field. Adopting this perspective, an advanced tool named FQ-IDCVT is used for the optimal sampling of these two-dimensional random functions. For highly correlated random fields, such as IM maps for any type of hazard, FQ-IDCVT ensures that the weighted ensemble of the samples tends to match particularly well all the properties of the field, including the correlation.

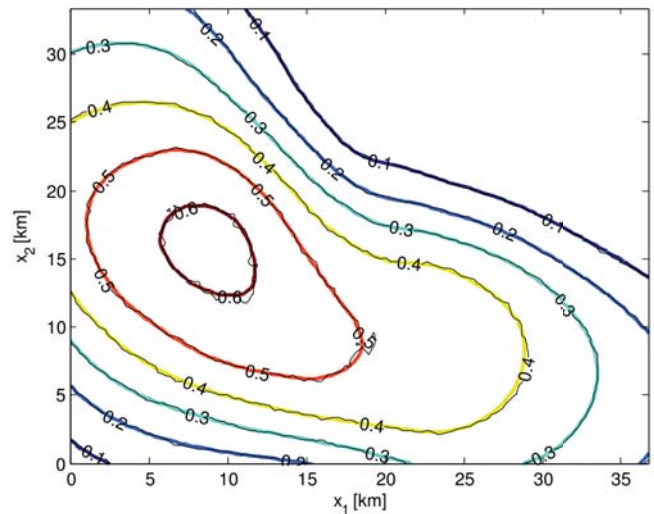


Figure 4: Comparison on the probability of exceedance $P[S_a(T = 0.1s) > 0.4g]$ between the exact (thick colored lines) and the result obtained from HQ with $N = 500$ (thin black lines).

6. REFERENCES

- Abrahamson, N., A. and Silva, W. J. (1997). "Empirical response spectral attenuation relations for shallow crustal earthquakes." *Seismological Research Letters*, 68(1), 94 – 127.
- Apivatanagul, P., Davidson, R., Blanton, B., and Nozick, L. (2011). "Long-term regional hurricane hazard analysis for wind and storm surge." *Coastal Engineering*, 58(6), 499 – 509.
- Bocchini, P. and Frangopol, D. M. (2011). "A stochastic computational framework for the joint transportation network fragility analysis and traffic flow distribution under extreme events." *Probabilistic Engineering Mechanics*, 26(2), 182–193.
- Bocchini, P., Miranda, M. J., and Christou, V. (2014). "Functional quantization of probabilistic life-cycle performance models." *Life-Cycle of Structural Systems: Design, Assessment, Maintenance and Management* (H. Furuta, D. M. Frangopol, M. Akiyama eds.), Tokyo, Japan, Taylor and Francis, 816–823.
- Christou, V., Bocchini, P., and Miranda, M. J. (2014). "Optimal representation of multi-dimensional random fields with a moderate number of samples." *Proceedings of CSM7* (Deodatis and Spanos eds.), Santorini, Greece, 1–12.
- Crowley, H. and Bommer, J., J. (2006). "Modelling seismic hazard in earthquake loss models with spatially distributed exposure." *Bulletin of Earthquake Engineering*, 4, 249–273.

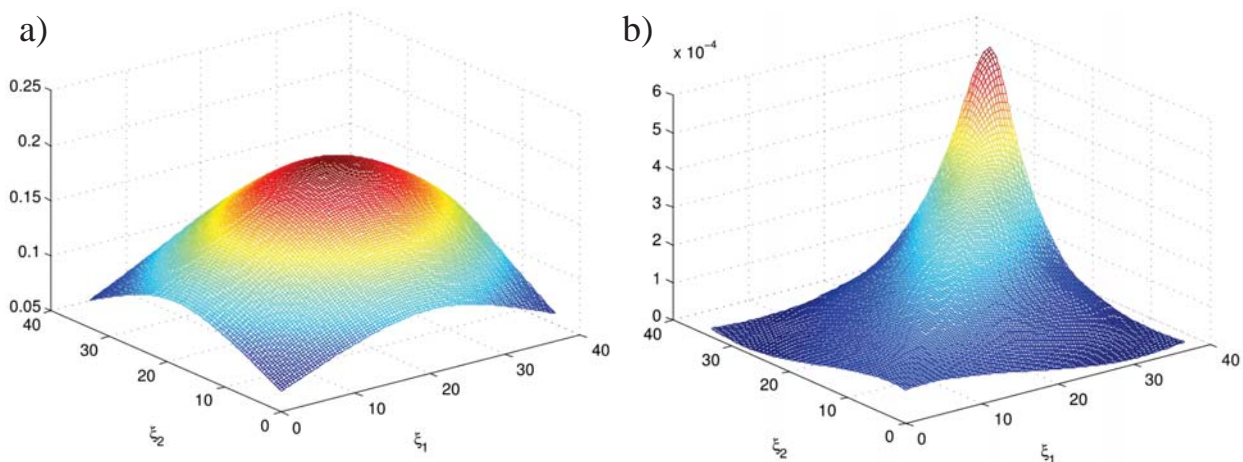


Figure 5: Approximation of the autocorrelation function of $S_a(T = 0.1)$ with $N = 500$ quantizers (a) and difference between approximated autocorrelation and exact (b).

- DHS (2003). *HAZUS-MH MR4 Earthquake Model Technical Manual*. Department of Homeland Security; Emergency Preparedness and Response Directorate; Federal Emergency Management Agency; Mitigation Division. Whashington, D.C.
- Emanuel, K., Ravela, S., Vivant, E., and Risi, C. (2006). “A statistical deterministic approach to hurricane risk assessment.” *Bulletin of the American Meteorological Society*, 87(3), 299–314.
- Gardoni, P., Mosalam, K., and Der Kiureghian, A. (2003). “Probabilistic seismic demand models and fragility estimates for rc bridges.” *Journal of Earthquake Engineering*, 7, 79–106.
- Grigoriu, M. (2009). “Reduced order models for random functions. Application to stochastic problems.” *Applied Mathematical Modelling*, 33(1), 161–175.
- Han, Y. and Davidson, R. A. (2012). “Probabilistic seismic hazard analysis for spatially distributed infrastructure.” *Earthquake Engng. Struct. Dyn*, 41, 2141–2158.
- Jayaram, N. and Baker, J. W. (2009). “Correlation model for spatially distributed ground-motion intensities.” 1687–1708.
- Jayaram, N. and Baker, J. W. (2010). “Efficient sampling and data reduction techniques for probabilistic seismic lifeline risk assessment.” *Earthquake Engng. Struct. Dyn*, 39, 1109–1131.
- Ju, L., Du, Q., and Gunzburger, M. (2002). “Probabilistic methods for centroidal Voronoi tessellations and their parallel implementations.” *Parallel Computing*, 28(10), 1477–1500.
- Kiremidjian, S., A., Stergiou, E., and Lee, R. (2007). “Issues in seismic risk assessment of transportation networks.” *Earthquake Geotechnical Engineering*, K. Pitilakis, D., ed., Springer Netherlands, 461–480.
- Lee, R. G. and Kiremidjian, A. S. (2007). “Uncertainty and correlation in seismic risk assessment of transportation systems.” *Report No. 2007/05*, Pacific Earthquake Engineering Research Center (PEER).
- Luschgy, H. and Pagès, G. (2002). “Functional quantization of Gaussian processes.” *Journal of Functional Analysis*, 196(2), 486–531.
- Miranda, M. J. and Bocchini, P. (2013). “Functional quantization of stationary gaussian and non-gaussian random processes.” *Safety, Reliability, Risk and Life-Cycle Performance of Structures and Infrastructures (G. Deodatis, B.R. Ellingwood, D. M. Frangopol eds.)*, Columbia University, New York, NY, CRC Press, Taylor and Francis Group, 2785–2792.
- Miranda, M. J. and Bocchini, P. (2015). “A versatile technique for the optimal approximation of random processes by functional quantization.” *Under review*.
- Moghtaderi-Zadeh, M. and Kiureghian, A. D. (1983). “Reliability upgrading of lifeline networks for post-earthquake serviceability.” *Earthquake Engng. Struct. Dyn*, 11, 557–566.
- Vaziri, P., Davidson, R., Apivatanagul, P., and Nozick, L. (2012). “Identification of optimization-based probabilistic earthquake scenarios for regional loss estimation.” *J. of Earthquake Engineering*, 16, 296–315.
- Vickery, P. J., Skerlj, P. F., Steckley, A. C., and Twisdale, L. A. (2000). “Hurricane wind field model for use in hurricane simulations.” *Journal of Structural Engineering*, 126(10), 1203–1221.